

Plant Communications, Volume 1

Supplemental Information

**A Thylakoid Membrane Protein Functions Synergistically with GUN5 in
Chlorophyll Biosynthesis**

Chi Zhang, Bin Zhang, Baicong Mu, Xiaojiang Zheng, Fugeng Zhao, Wenzhi Lan, Aigen Fu, and Sheng Luan

1 Supplemental Materials

2

3

4

5

6

7

8

9

10

11

12

13

14

15

16

17

18

19

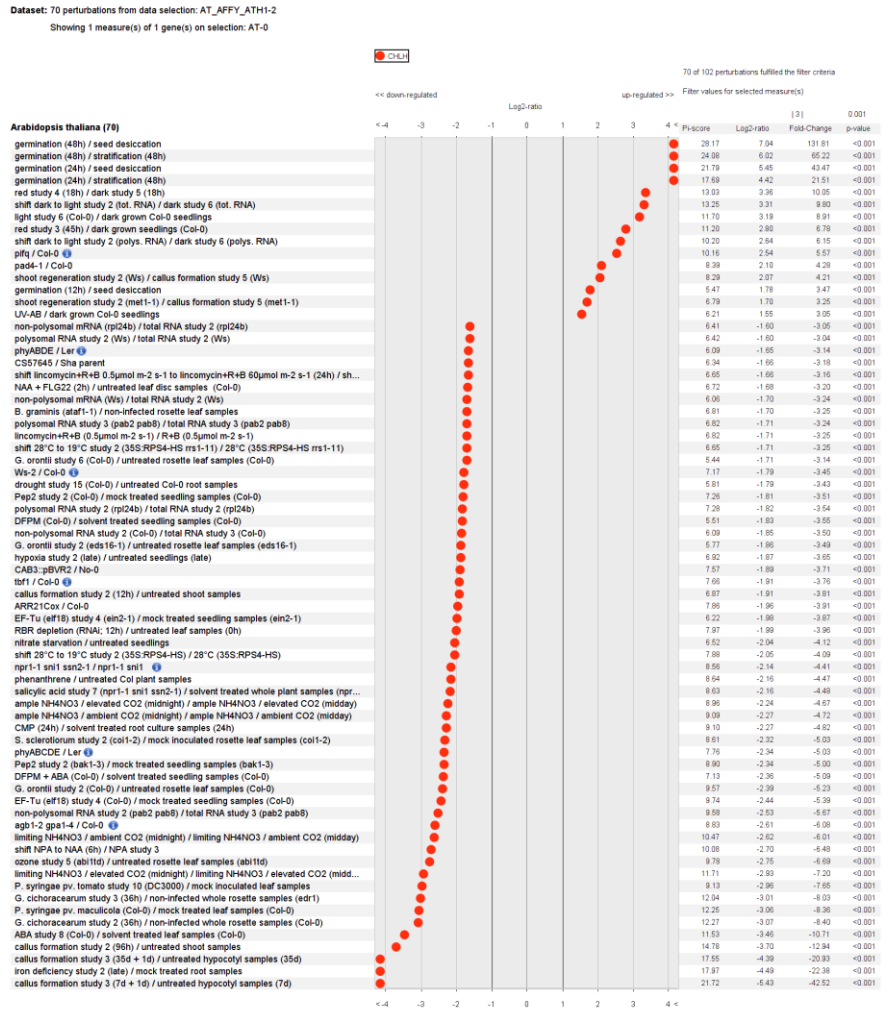
20

21

22

23

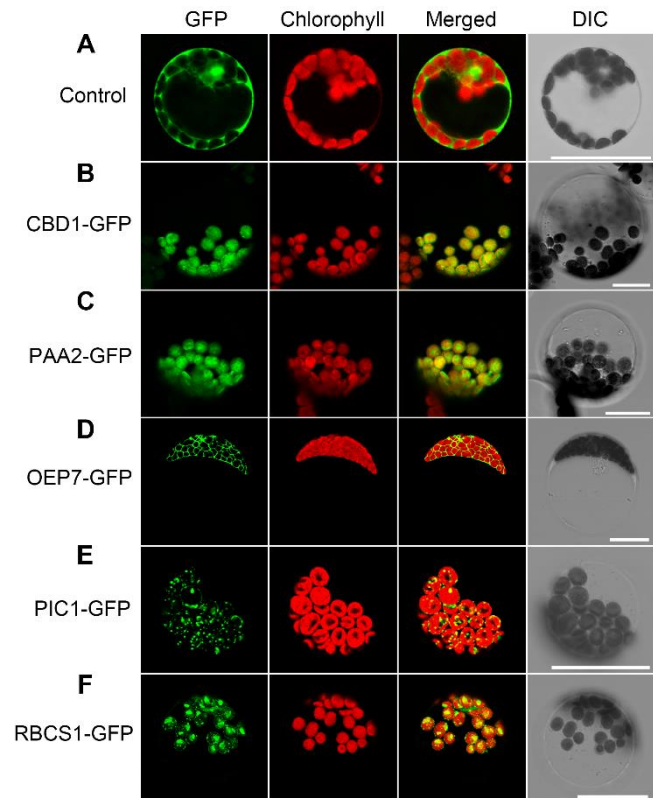
24



Supplemental Figure 1. Expression Profiles of *CHLH/GUN5* under Perturbation Conditions.

The dataset were 70 perturbations which the expression profiles of *CHLH/GUN5* were most regulated. Data were collected from the Genevestigator database.

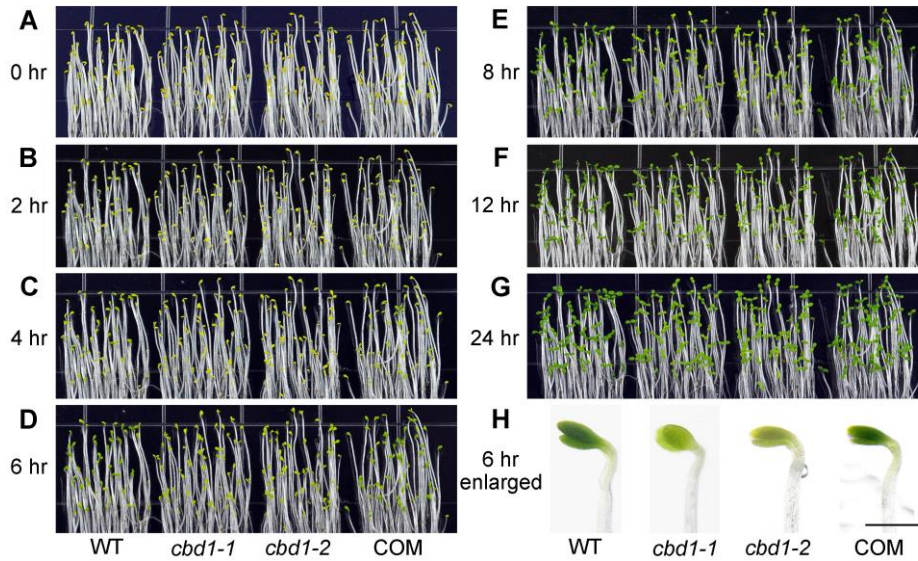
25
26
27
28
29
30
31
32
33
34
35
36
37
38



39 **Supplemental Figure 2. Subcellular Localization of CBD1 and Marker Proteins**
40 **in Chloroplast.**

41 *Arabidopsis* leaf protoplasts were transformed with plasmids that express the
42 indicated gene constructs under control of the constitutive 35S Cauliflower mosaic
43 virus promoter. **(A)** The unfused GFP vector served as a control. **(B)** The GFP coding
44 sequence was fused to the C terminus of the CBD1 coding region in the pEZSNL
45 vector. **(C-F)** Fluorescence signals of marker proteins localized in different
46 compartments of chloroplast. PAA2-GFP, PIC1-GFP, OEP7-GFP, and RBCS1-GFP
47 were used as markers of thylakoid membrane, inner envelope, outer envelope, and
48 stroma respectively. After 16 h of expression, protoplasts were observed using a
49 confocal laser scanning microscope. Green fluorescence signals, chlorophyll red
50 auto-fluorescence, merged signals from GFP and chlorophyll channels, and
51 bright-field images that showed intactness of the protoplasts are shown separately
52 from left to right in each lane. Scale bars, 20 μ m.

53
54



55

56

57 **Supplemental Figure 3. *cbd1* Exhibited a Slower Rate in Chl Biosynthesis.**

58 (A) to (G) 3-day-old dark-grown etiolated WT, *cbd1-1*, *cbd1-2*, and COM seedlings

59 exposed to continuous light for indicated time periods. Scale bar, 1 cm. (H) Enlarged

60 representative WT, *cbd1-1*, *cbd1-2*, and COM seedling after light exposure for 6 h.

61 Scale bar: 1 mm.

62

63

64

65

66

67

68

69

70

71

72

73

74

75

76

77

78

79

80

81

82

83

84

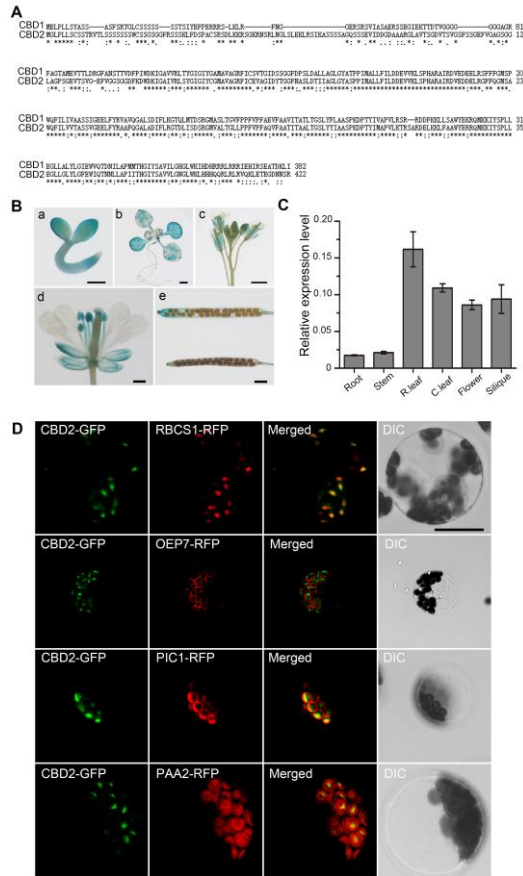
85

86

87

88

89



90 **Supplemental Figure 4. Expression Profiles of *CBD2* and Subcellular**
91 **Localization of *CBD2*.**

92 (A) Sequence alignment of CBD1 and CBD2 using Clustal X. (B) GUS staining of
93 (a-c) 1-3 days old seedlings after germination, (d) Inflorescence and silique from
94 4-week-old plants, and (e) Rosette leaf from 3-week-old plants in soil. Scale bars, 200
95 μm in (a) and (b), 1 mm in (c) and (f), 2 mm in (d) and (e). Data are mean ± SD. n = 4.
96 (C) Relative expression levels of *CBD2* in various tissues are revealed by qRT-PCR
97 analysis. (D) The construct of *35S::CBD2-GFP* was co-transformed with the marker
98 RBCS1-RFP (stroma), OEP7-RFP (outer envelope), PIC1-RFP (inner envelope), or
99 PAA2-RFP (thylakoid membrane) into *Arabidopsis* leaf protoplasts for fluorescence
100 observation using confocal laser scanning microscope after 16 h of expression. Green
101 fluorescence signals, chlorophyll red auto-fluorescence, merged signals from GFP and
102 chlorophyll channels, and bright-field images that showed intactness of the
103 protoplasts are shown separately from left to right in each lane. Scale bar, 20 μm.

104

105

106

107

108

109

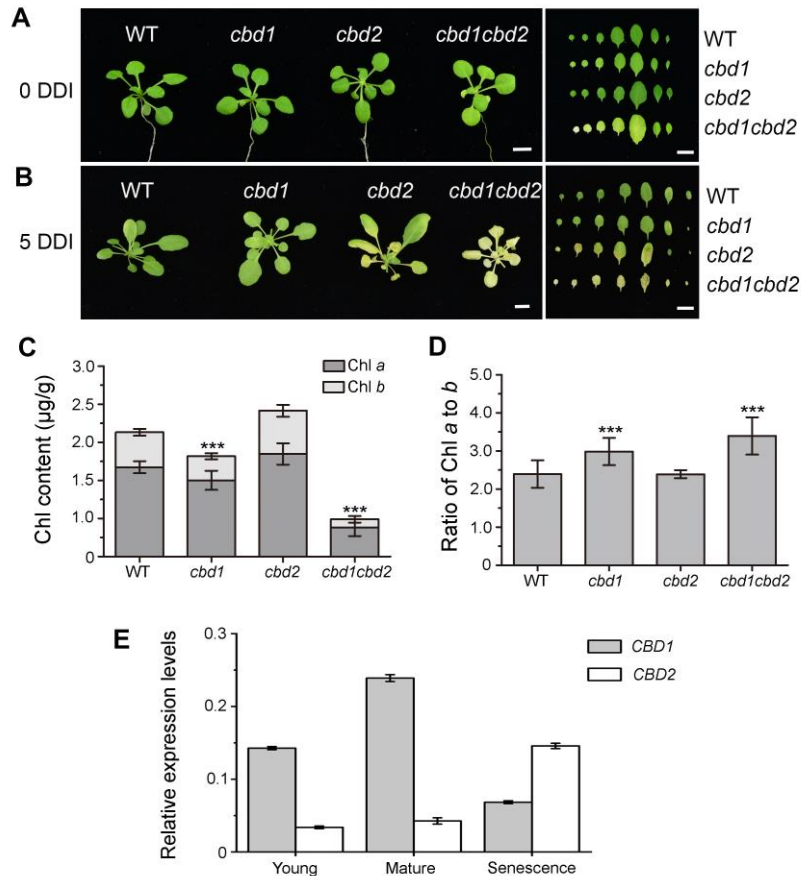
110

111

112

113

114



115 **Supplemental Figure 5. Phenotypic Analysis of WT, *cbd1*, *cbd2*, and *cbd1cbd2***
 116 **Mutants.**

117 (A) 3-week-old WT, *cbd1*, *cbd2*, and *cbd1cbd2* mutant grown in normal conditions.
 118 Detached leaves were shown in the right. (B) 3-week-old WT, *cbd1*, *cbd2*, and
 119 *cbd1cbd2* mutant were dark incubated for 5 days. Detached leaves were shown in the
 120 right. Scale bars, 1 cm. (C) Chlorophyll content and (D) ratio of Chl *a* to *b* of
 121 seedlings in (A) (Student's *t* test, *** $P < 0.001$). (E) Relative expression levels of
 122 *CBD1* and *CBD2* in leaves of different ages were detected by qRT-PCR analysis.
 123 Young leaves: the two leaves that newly emerged; mature leaves: the middle leaves;
 124 senescence leaves: the two true leaves close to the base of plants.

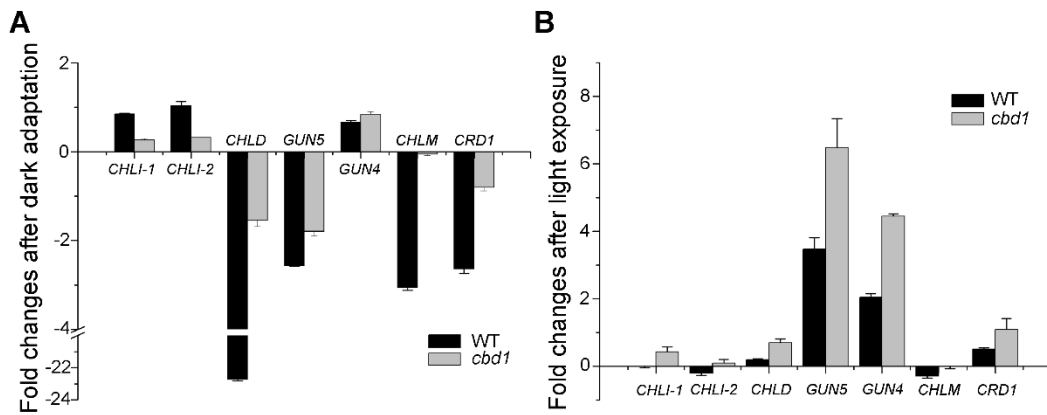
125

126

127

128

129



131 **Supplemental Figure 6. Altered Expression Levels of Genes Encoding Key**
 132 **Enzymes in Chl Biosynthetic Pathway.**

133 (A) 3-week-old WT and *cbd1* were dark-adapted for 1 hour before harvest. (B)
 134 Dark-grown WT and *cbd1* were harvested after 1 hour light exposure. Data are mean
 135 \pm SD, n=4. *Actin2* was used as an internal reference.

136

137

138

139

140

141

142

143

144

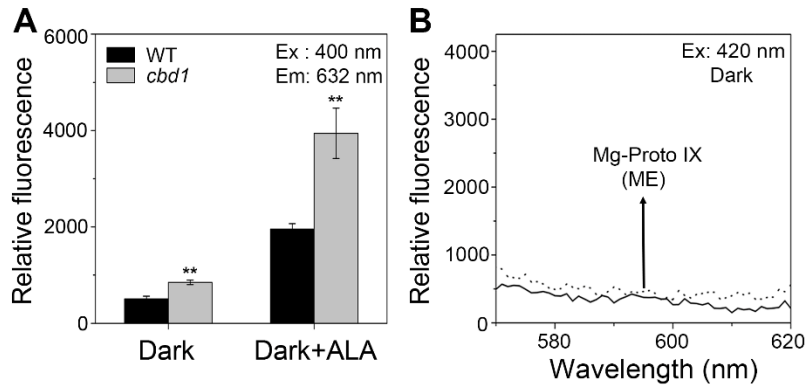
145

146

147

148

149



150

151

152 **Supplemental Figure 7. Spectrofluorometric analysis of Chl precursors.**

153 (A) Levels of Proto IX in dark-adapted WT and *cbd1* seedlings are determined by
 154 spectrofluorometry. 3-week-old seedlings were dark-adapted for 3 days before
 155 harvested for measurement. For ALA treatment, 10 mM ALA was added. Excitation at
 156 400 nm produces an emission peak at 632 nm corresponding to the Proto IX content.

157 (B) In dark-adapted seedlings, excitation at 420 nm did not produce an emission peak
 158 at 595 nm, indicating that the no Mg-Proto IX (ME) was detected by
 159 spectrofluorometry in this condition. Data are mean \pm SD. n=4. Asterisks indicate
 160 statistically significant differences compared with the wild type (Student's *t*-test,
 161 ** $P < 0.01$).

162

163

164

165

166

167

168

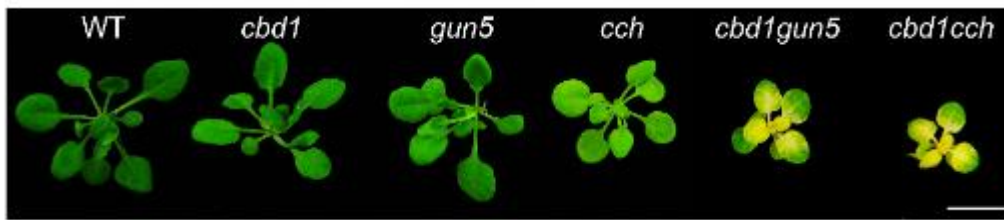
169

170

171

172

173



174 **Supplemental Figure 8. Double Mutant *cbd1gun5* and *cbd1cch* Exhibits the Same**
175 **Phenotype.**

176 3-week-old WT and mutant lines grown in half-strength MS medium. Scale bar, 1 cm.

177

178

179

180

181

182

183

184

185

186

187

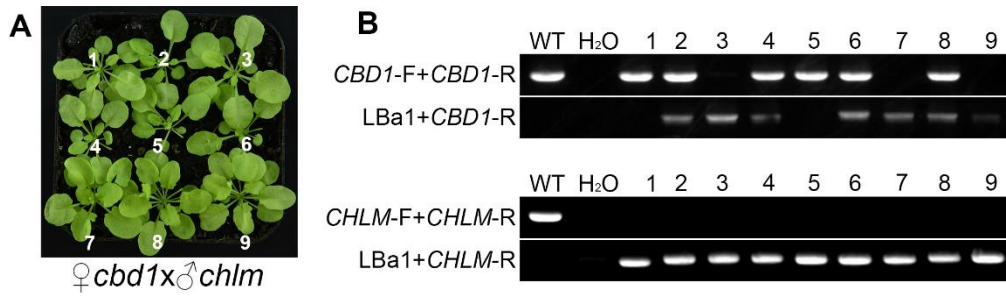
188

189

190

191

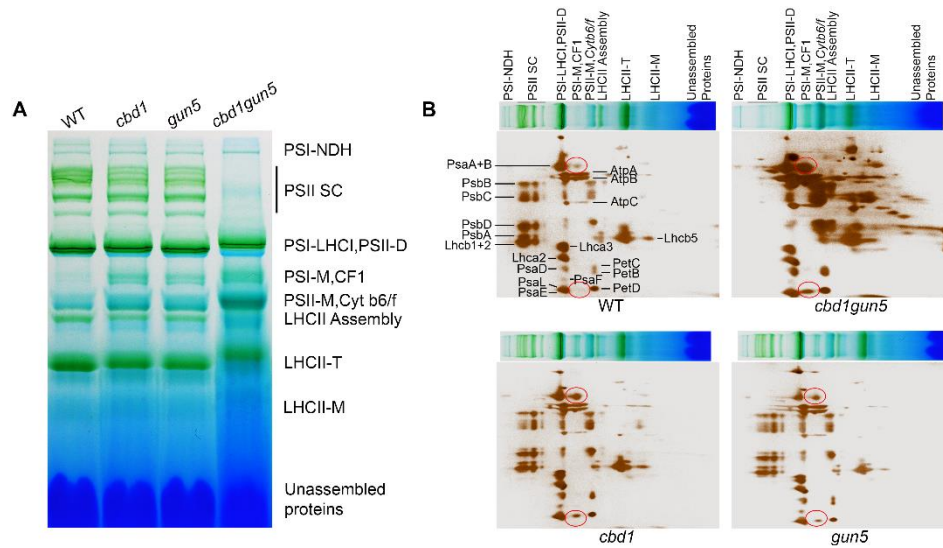
192



193 **Supplemental Figure 9. Identification and phenotype of *cbd1chlm* double**
 194 **mutant.**

195 (A) Nine *cbd1chlm* double mutant lines grown in soil in greenhouse. (B) PCR
 196 amplification of *CBD1* and *CHLM* genomic fragment from WT and the nine mutant
 197 lines. Primer pair *CBD1*-F and *CBD1*-R was used to amplify genomic fragment of
 198 *CBD1*. Primer pair *CBD1*-R and LBa1 (the T-DNA left border flanking sequence) was
 199 used to identify T-DNA insertion in *CBD1*. Primer pair *CHLM*-F and *CHLM*-R was
 200 used to amplify genomic fragment of *CHLM*. Primer pair LBa1 and *CHLM*-R was
 201 used to identify T-DNA insertion in *CHLM*. Wild type (WT) was used as a positive
 202 control and water was used as a negative control (H₂O).

203
 204
 205
 206
 207
 208
 209
 210
 211
 212
 213
 214
 215
 216



218 **Supplemental Figure 10. Disturbed Organization of Thylakoid Membrane**
 219 **Protein Complexes in Mutants.**

220 (A) BN-PAGE analysis of equal thylakoid proteins (10 μ g chlorophyll) of 3-week-old
 221 WT, *cbd1*, *gun5*, and *cbd1gun5* grown in half-strength MS. Thylakoid membranes
 222 were solubilized with 1% DM by 5%-13.5% gradient gel. Designation of thylakoid
 223 membrane protein complexes are labeled to the right. Six biological replicates were
 224 performed and a representative one is shown. (B) 2D-SDS-PAGE fractionation of
 225 thylakoid membrane protein complexes. After separation in the non-denaturing
 226 gradient gel in the first dimension, the gels were sliced and laid on the top of the
 227 denaturing 12.5% 2D SDS-PAGE gel for the further separation in the second
 228 dimension. The followed silver stain was applied for the visualization of specific
 229 proteins. The red oval circle indicates the location of PsaA+B and Psa E proteins.

230

231

232

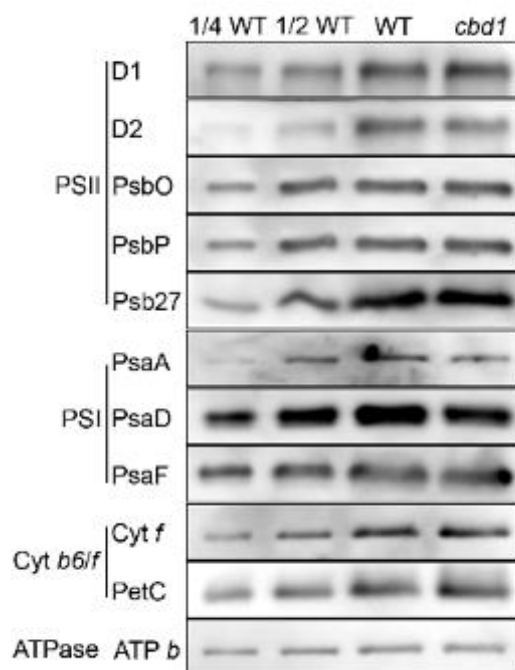
233

234

235

236

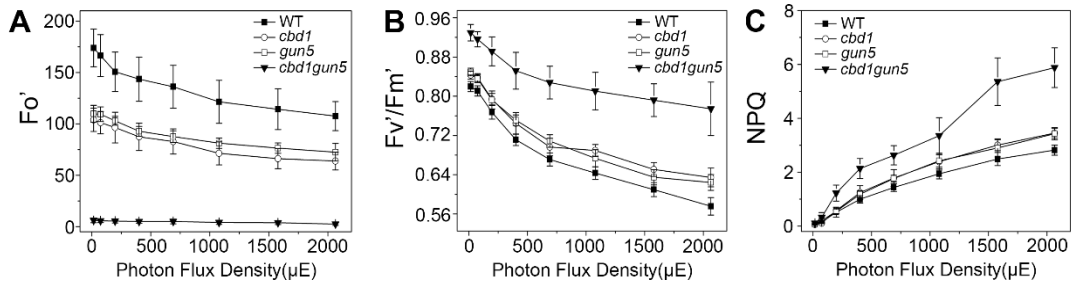
237
238
239
240
241
242
243
244
245
246
247
248
249
250
251
252
253
254
255
256
257
258
259
260
261
262
263
264



Supplemental Figure 11. Immunoblotting Analysis of Subunits in Photosynthetic Supercomplexes.

SDS-PAGE immunoblotting analysis of thylakoid proteins (1 μ g chlorophyll) from WT and *cbd1*. Antibodies were applied as indicated.

265



266

267 **Supplemental Figure 12. Photosynthetic Activity of PSII in WT, *cbd1*, *gun5*, and**
268 ***cbd1gun5*.**

269 Chlorophyll *a* fluorescence parameters of 3-week-old WT, *cbd1*, *gun5*, and *cbd1gun5*.
270 Plants were dark-adapted for 40 min before measurement. **(A)** F_o' : the minimal
271 fluorescence; **(B)** F_v'/F_m' : the PSII maximum efficiency; **(C)** NPQ: the
272 non-photochemical quenching. Data are mean \pm SD. n = 5.

273

274

275

276

277

278

279

280

281

282

283

284

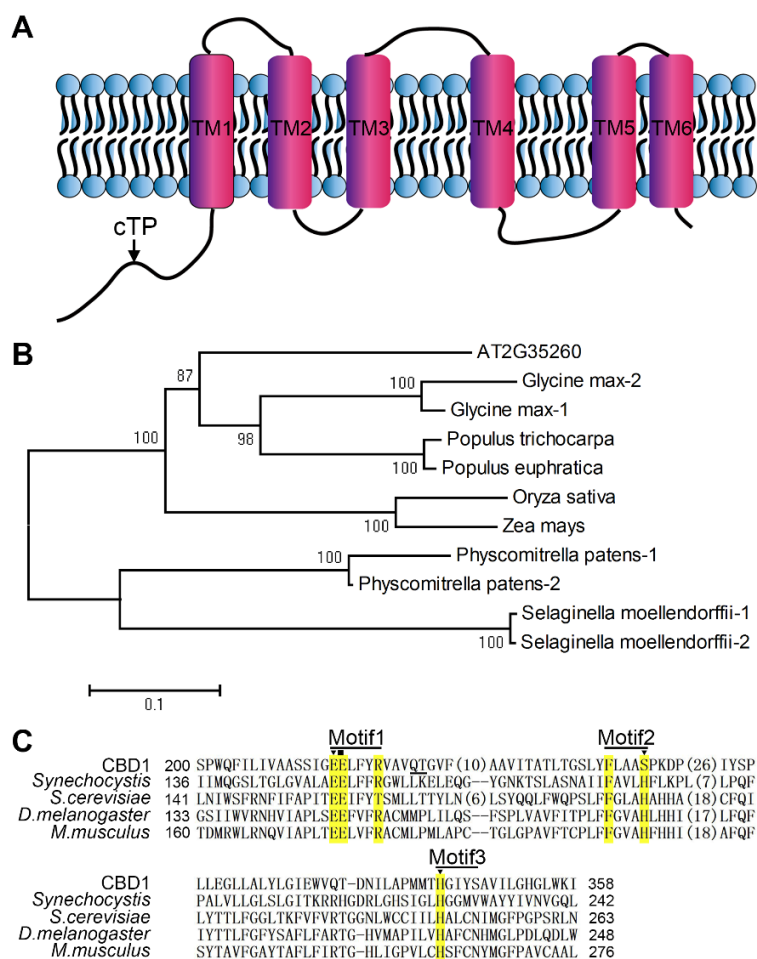
285

286

287

288

289
290
291
292
293
294
295
296
297
298
299
300
301
302
303
304
305
306
307
308
309
310
311
312
313
314
315
316
317



Supplemental Figure 13. Phylogenetic Analysis of CBD1.

(A) Predicted topology structure for CBD1 based on the TMHMM Server v.2.0. (<http://www.cbs.dtu.dk/services/TMHMM/>). (B) The phylogenetic tree was constructed using the Neighbor-Joining method based on the Poisson model of MEGA 6. Bootstrap values (1000 replicates) were shown for corresponding nodes. The analysis involved 11 amino acid sequences (*Arabidopsis thaliana*, AT2G35260; *Populus euphratica*, XP_011018585.1; *Populus trichocarpa*, XP_006368412.1; *Oryza sativa*, XP_015633215.1; *Glycine max*, NP_001239886.1; *Glycine max*, KRH77201.1; *Physcomitrella patens*, XP_001769984.1; *Physcomitrella patens*, XP_001764584.1; *Selaginella moellendorffii*, XP_002967687.1; *Selaginella moellendorffii*, XP_002964348.1; *Zea mays*, NP_001137056.1). (C) Multiple sequence alignment of CBD1 with its Type II CAAX homologues (Pei and Grishin, 2001).

318

319 **Supplemental Table 1. Metal Ion Content Analysis**

320

321

Genotype	Fraction	Fe	Mn	Cu	Ca
WT	Leaf	0.13±0.02	0.11±0.02	0.02±0.002	28.23±1.19
<i>cbd1</i>	Leaf	0.13±0.01	0.11±0.01	0.02±0.001	29.24±2.25
WT	Thylakoid	7.16±1.81	1.58±0.06	0.54±0.02	15.10±5.14
<i>cbd1</i>	Thylakoid	6.99±1.77	1.22±0.02	0.49±0.03	13.16±2.30

322 Metal ion contents were measured for leaves of wild-type and *cbd1* plants grown on
323 soil as well as for intact thylakoids isolated from these plants. Values indicate amounts
324 of metal ions ($\mu\text{g}/\text{mg}$ dry weight for leaf fractions, $\mu\text{g}/10^9$ thylakoids for intact
325 thylakoids). All values are averages of four replicates \pm SD.

326

327

328

329

330

331

332

333

334

335

336

337

338

339

340

341

342

343

344 **Supplemental Table 2. Primers Used in This Study**

345

Primer Name	Prime Sequence (5'-3')	Application
CBD1-F	CGGGATCCATGGAGCTTCCGTTACTCTCGTAG	Mutant identification
CBD1-R	GGAATTCTTAAATCAACTTATCCGTGGCCTCCG	
Lba1	TGGTTCACGTAGTGGGCCATCG	
gun5-point-F	GGTGGTCATGGACAACGAAC	
gun5-point-R	CCAAAGAACCTGCCCAAGAG	
chlm-F	GCTTTCAGACTGTGTTCCAATTG	
chlm-R	CCATAGCAGCAGAAATATCGG	
CBD1-genomic-F	CGGGATCCTGCTAAGTATTTTTAGTTTACCTAG	Genomic complementation
CBD1-genomic-R	CGCTGCAGGCAGGGCACAAAGCAC	
CBD1-GFP-F	GGAATTCGATGGAGCTTCCGTTACTCTCGTAG	Subcellular localization
CBD1-GFP-R	CGGGATCCGCAATCAACTTATCCGTGGCCTCCG	
CBD2-GFP-F	GGAATTCGATGGGTCTTCCTTTATTGTCTTGTAGTTCC	
CBD2-GFP-R	CGGGATCCGCTCTTGAGTTGTTGTCACCTTCAGTTTCAAG	
PAA2-GFP-F	CGGGTACCATGGCGAGCAATCTTCTCC	
PAA2-GFP-R	CGCCCGGGTAGATGCTTGAAGCTTTGCTCTTT	
PIC1-GFP-F	CGCTCGAGATGCAATCACTACTCTTGCCG	
PIC1-GFP-R	CGGGATCCAGAGCAACCTTAGGAACTACGAC	
OEP7-GFP-F	CGCTCGAGATGGGAAAACTTCGGGAGC	
OEP7-GFP-R	CGGGATCCAGCAAACCTCTTTGGATGTGG	
RBCS1-GFP-F	CGCTCGAGATGGCTTCCTCTATGCTCTC	
RBCS1-GFP-R	CGGGATCCACACCGGTGAAGCTTGGTGG	
CBD1pro-F	CCCAAGCTTTGCTAAGTATTTTTAGTTTACCTAG	
CBD1pro-R	CGGGATCCTGAAGTTATTCGAAGTAACCG	
CBD2pro-F	CCCAAGCTTCTTTGTAATAAAGCAATTTAATGATG	
CBD2pro-R	CGGGATCCTTATAACATGCGACAACTCTCAG	

CBD1-M-F	GGAATTCATGGAGCTTCCGTTACTCTCG	MM281 complementa tion
CBD1-M-R	CGGGATCCTTAAATCAACTTATCCGTGGCCT CC	
CBD1-Q-F	ACGGAGCAGTGAAGGGATTG	qRT-PCR
CBD1-Q-R	TCAACGGTGGTGGAGTTAGC	
CBD2-Q-F	TTGACTGGACTCTTGCCACC	
CBD2-Q-R	GAGAGAACCAGTGAGAGCGG	
GUN4-Q-F	CACTTACCGCTCACAAACGC	
GUN4-Q-R	GCTCCTACTCCTGCCTGTTT	
CHLI-1-Q-F	ACCCGGCGAGGTTTATCTTG	
CHLI-1-Q-R	GCTTGTCCTGCTCGGTTTTG	
CHLI-2-Q-F	GCTGCATCTGGTTGGAACAC	
CHLI-2-Q-R	TTAACTCTCAGCTCGGCGTC	
CHLD-Q-F	TCCCTCCCCAAACGAAACAG	
CHLD-Q-R	AGGGAAAAACTGTCGGCCAT	
CHLH-Q-F	GCTTACCTCGCTTCTTGGGT	
CHLH-Q-R	CCACCAACTTCAGGCACTCT	
CHLM-Q-F	CGTTTGCTCCTTCCTTGTTGTC	
CHLM-Q-R	CCGAGTACGGCGATTGTTGT	
CRD1-Q-F	CCCAAAGCTCTCAAACCCGA	
CRD1-Q-R	TCGTTCCCTTCTTGGACTTCG	
Actin2-F	ACTCTCCCGCTATGTATGTCGCC	
Actin2-R	ATTTCCCGCTCTGCTGTTGTGGT	
CBD2 _{CRISPR} -F	CGTGTAGACATGCAAAGTGGT	CRISPR
CBD2 _{CRISPR} -R	CCTTCTTACAGACATGTGCC	
CBD2gRT1+	CCTGAATCCATTCAAAGCCGGTTTTAGAGCT AGAAAT	
CBD2gRT2+	GATCGACGACGGAGATGCGGGTTTTAGAGC TAGAAAT	
CBD2gRT3+	GGGAGACTTTGGACCGTTGGAGTTTTAGAGCT AGAAAT	
CBD2-AtU6-2 9-T1	CGGCTTTGAATGGATTTCAGGCAATCTCTTAG TCGACT	
CBD2-AtU3b- T2	CCGCATCTCCGTCGTCGATCTGACCAATGTT GCTCC	
CBD2-AtU3d- T3	TCCAACGGTCCAAAGTCTCCTGACCAATGGT GCTTTG	